Characterisation of demoulding parameters in micro-injection moulding

Dimov, Stefan; Griffiths , Christian; Tosello, Guido; Scholz, Steffen; Rees, Andrew; Whiteside, Ben

[Link to publication on Research at Birmingham portal](#)

Characterisation of demoulding parameters in micro-injection moulding

C.A. Griffiths[a], G.Tosello[b], S.S. Dimov[c], S.G. Scholz[d], A. Rees[e], B. Whiteside[f]

[a] School of Mechanical, Aerospace and Civil Engineering, *The University of Manchester, Manchester, UK*

[b] *Department of Mechanical Engineering, Technical University of Denmark, Kgs. Lyngby, Denmark*

[c] *School of Mechanical Engineering, Birmingham University, Birmingham, UK*

[d] *Institute for Applied Computer Science, Karlsruhe Institute of Technology, Karlsruhe, Germany*

[e] *College of Engineering, Swansea University, Swansea SA2 8PP, UK*

[f] *Centre for Polymer Micro and Nano Technology, University of Bradford, Bradford, UK*

Abstract

Condition monitoring of micro injection moulding is an effective way of understanding the processing effects of variable parameter settings. This paper reports an experimental study that investigates the characteristics of the demoulding behaviour in micro injection moulding (μ-IM) with a focus on the process factors that affect parts' quality. Using a Cyclic Olefin Copolyme (COC) microfluidics demonstrator, the demoulding performance was studied as a function of four process parameters (melt temperature, mould temperature, holding pressure and injection speed), employing the design of experiment approach. The results provide empirical evidences on the effect that processing parameters have on demoulding conditions in μ-IM, and identifies combinations of parameters that can be used to achieve the optimal processing conditions in regards to demoulding behaviour of micro parts. It was concluded that there was a direct correlation between the applied pressure during part filling, holding phases and the demoulding characteristic factors of the μ-IM cycle such as ejection force, integral and time.

Notations

ANOVA - Analysis of Variance

ABS - Acrylonitrile Butadiene Styrene

COC - Cyclic Olefin Copolymer

d - Measuring Pin Diameter

DOE - Design of Experiments

F^e - Demoulding Force

F^e_{max} - Maximum Demoulding Force

F^e_{work} - Demoulding Force Work

F^e_{rate} - Demoulding Force Rate

IM - Injection Moulding

OA - Orthogonal Array

PC – Polycarbonate

PVT – Pressure Volume Temperature

P_h - Holding Pressure

S/N – Signal to Noise Ratio

SV_R - Surface to Volume Ratio

t - Time

T_b - Melt / Barrel Temperature

t_h - Holding Pressure Time

T_m – Mould / Tool Temperature

T_g - Glass Transition Temperature

V_i - Injection Speed

Δt - Time Step of Data Acquisition System

δ - Relative Effect

σ - Standard Deviation

μ-IM - Micro-Injection Moulding

Keywords: micro injection moulding, process monitoring, demoulding.

1. Introduction

Healthcare, automotive, communication and consumer electronics industry needs are driving demand for lighter, thinner, and smaller device components. As a result, injection moulding (IM) of thin-wall polymer parts faces new challenges in every aspect of the process, including requirements for high productivity, advanced mould cavity engineering technologies and precise process control [1]. Dedicated micro-injection moulding technologies have emerged from these requirements and there are now a number of machines available which are optimised for micro-component production. These new processes have a range of benefits over their standard injection moulding cousins including lower energy costs (raw material production, process power) and in many cases improved functionality and simplified integration of ancillary processes such as product handling, inspection and packaging. Despite these technological advances, successful implementation of micromoulding processes remains challenging and exploratory work has revealed that the effects of variations in process control and/or repeatability in relation to some critical process design parameters have to be investigated systematically. In particular, the higher pressure needed to fill parts requires advanced IM machines [2], and plastic materials experience a rapid increase and then decrease of temperature and pressure during the moulding process. This leads to solidification, and locking of residual stresses, orientation, and other part properties that determine the quality of the moulded part [3].

Microfluidic or 'Lab-on-a-Chip' (LoC) systems have many industrial applications especially in pharmacy and biotechnology e.g. for substance screening and point of care medical diagnostics. Micro injection moulding (μ-IM) processes are highly suited for high volume manufacture of these devices which are inexpensive and light weight, and can be considered as disposable alternatives to ceramic platforms. Cyclic olefin copolymer (COC) is one of the polymers that are suitable for producing microfluidics parts because of its high glass transition temperatures (T_g), low moisture uptake, high chemical

resistance, excellent optical properties, bio-compatibility, sterilization possibility and thus suitability for medical approval [4,5,6].

µ-IM has been applied successfully in this study to manufacture microfluidics platforms with micro-channel arrays down to 50 µm in size. The replication accuracy of moulded parts in COC polymer resin has proved successful due to its low viscosity and low isotropic shrinkage [7]. However, determining the optimum process conditions for mass replication becomes the key to improving the part quality. DVD-R substrate and blu-ray Discs for example that are injection moulded in 4 s or less, incorporate new high resolution micro/nano surface structures, and specific quality requirements have to be satisfied in regard to microgroove depth, duplication accuracy, birefringence, diffraction efficiency and warpage [8,9].

In this paper, the effect of processing parameters on the demoulding characteristics of a microfluidic part is reported. The paper is organised as follows. The next section describes the effects of temperature and pressure on part demoulding. Then, the experimental set-up including mould and part designs and µ-IM machine used to investigate demoulding forces is described. Finally, the research findings are presented and the interdependences between process factors and demoulding parameters in µ-IM are discussed and conclusions are drawn.

2. The effects of process conditions on part demoulding

Dimensional consistency is a critical attribute of IM part quality and is highly dependent on the processing parameters. In µ-IM, higher mould temperatures can be adopted to improve moulding performance and for very demanding microfeatures and structures, mould temperatures are set to be higher than the T_g of the polymer, which increases the filling ratio significantly, and has a favourable effect on the replication of microstructures [10,11]. During the cooling stage of the IM process polymer materials experience volume variations when they undergo temperature changes, these variations are a result of the polymer pressure-volume-temperature (pvT) behaviour. The

dimensional shrinkage can be estimated by knowing the pvT of the polymer. However, there has been an increasing recognition that cavity pressure measurements and control of the polymer state are necessary to establish experimentally the pvT behaviour, hence the actual shrinkage ranges [12]. Condition monitoring of pressure during the IM process is a technique that can be used to compensate the effects of shrinkage and thus ensure that pressure in the cavity can be maintained. The predictions and monitoring of cavity pressure are especially important for thin wall parts where the pressures can be high enough to cause tool deformation by flexuration or compression of the mould material [13 14].

For typical µ-IM high injection velocity can be applied to prevent early polymer solidification caused by the inherent rapid melt cooling associated with the process. Alternatively, maintaining high mould temperature during the filling process can lead to reduction in the maximum cavity pressure (P_{max}) but an increase in the overall pressure over time (P_{work}), and be dependent on the polymer material used. In the research conducted by Chen et al., a heating system was used to control the mould surface temperature in µ-IM of biochips with micro-channel arrays that led to improvements of replication accuracy at higher settings of mould temperature [16]. An analytical model was developed by Lin et al., to predict the filling of nano structures in µ-IM. The research demonstrated that a higher mould temperature (T_m) leads to better filling. The research also concluded that filling is limited to below 100 nm for mould temperatures in the range of 40-75 °C and at temperatures of 100 °C filling between 400 - 500 nm can be achieved. In addition, if the aspect ratio of the nano/micro structures is higher than 1, T_m should be raised near or above T_g of the polymer [10].

An investigation by Griffiths et al. concluded that the introduction of polymer part stresses before demoulding can result in a considerable amount of elastic deformation after demoulding. Through Taguchi analysis optimum process parameters were developed with regards to ejection force reduction [15]. Especially, it was reported that for Polycarbonate (PC) and Acrylonitrile Butadiene Styrene (ABS), mould temperature was the process parameter with

the highest percentage contribution, with increasing values resulting in reduced ejection force [17].

Ong et al., found that the replication of a micro lens array using high mould temperatures was not favourable, due to the increase in extensibility of plastic, which led to distortion and extension of the lens profiles [18]. Further research on IM parts with micro channels with widths of 30, 60, and 100 μm concluded that using optimum settings for mould temperature and hold pressure, the channels were completely replicated whilst a higher injection pressure caused excessive stress during demoulding [19, 20].

Both high surface to volume ratio (SV_R) and high aspect ratio micro features are a major challenge in μ-IM and require effective solutions in order to improve part quality. Optimum parameter settings within the processing window for a given polymer are required to ensure that all functional features are fully replicated and also the part demoulding forces are minimised. The effects of melt temperature on the cavity filling and the rate of thermal conduction until ejection temperature is reached, during the cooling stage of the process have to be investigated in order to facilitate part production without introducing any part deformation.

3. Condition monitoring

3.1 Demoulding force (F^e) curves

The focus of this research is on the demoulding force and its associated characteristic parameters in μ-IM. To acquire the necessary information about F^e, a force transducer is positioned behind an ejector pin to indirectly measure F^e during each injection cycle. The recorded F^e curves as shown in Figure 1 provide information about the demoulding stage of the injection moulding cycle. Especially, of interest is the demoulding force rate (F^e_{rate}), maximum demoulding force (F^e_{max}), the demoulding force work (F^e_{work}) that the parts can experience, as well as the ejection time (defined as the time during which the ejection force is active). The demoulding F^e force can be calculated using the cavity pressure P^c curve as follows:

$$F^e = P^c / A \qquad\qquad (1)$$

(where A is the projected area of the cavity pressure sensor in contact with the polymer melt flow).

To compare demoulding force curves their characteristic numbers can be calculated. In this research the following five characteristic numbers were investigated: maximum ejection force (F^e_{max}), ejection force work (F^e_{work}), ejection force rate (F^e_{rate}), total ejection time (t^e), average ejection force in the second phase of the ejection cycle, i.e. after F^e_{max} (F^e_2). The software Matlab™ was employed to calculate these key values, while a t series' function provided the key variables as outlined below to determine the F^e conditions. F^e_{max} represents the maximum demoulding force during the demoulding stage of a μ-IM cycle:

$$F^e_{\;max} = F^e(t_{max}) = max\left(F^e(t)\right) \qquad\qquad (2)$$

F^e_{work} is determined by F^e over time, t, and thus is defined by the integral value begining with F^e at the start of the demoulding stage and ending with F^e_{max}. The F^e curve is defined with discrete values, the number of which depends on the sampling rate of the data acquisition system, while F^e_{work} is a sum of F^e over a time interval starting with t_{start}. The time step Δt for recording F^e was 1 ms, determined by the 1 kHz sampling rate of the data acquisition system. Thus, the F^e_{work} value was calculated employing the following equation:

$$F^e_{\;work} = \left(\sum_{t=t_{start}}^{t_{end}} F^e(t) \right) \cdot \Delta t \qquad\qquad (3)$$

The demoulding force rate of change represents the average gradient of F^e between the starting threshold and F^e_{max}. Especially, it starts when F^e reaches a value that is 10% above the starting threshold while ends 10% below F^e_{max}.

$$F^e_{rate} = \frac{0.9 \cdot F^e_{max} - 1.1 \cdot F^e_{start}}{t_{Slope\_end} - t_{Slope\_start}} \qquad (4)$$

where t $_{slope\_start}$ and t $_{slope\_end}$ represent the corresponding times to the starting and the end value of F^e. Figure 1 shows the characteristic numbers in the context of the F^e curve.

Ejection time (t^e), i.e. the time elapsed between the moment of the starting threshold of F^e and the end of the demoulding phase (F^e=0). Average ejection force in the second phase of the ejection cycle (F^e_2), defined as the average force in the time interval between the time at which F^e_{max} is reached and end of the demoulding phase.
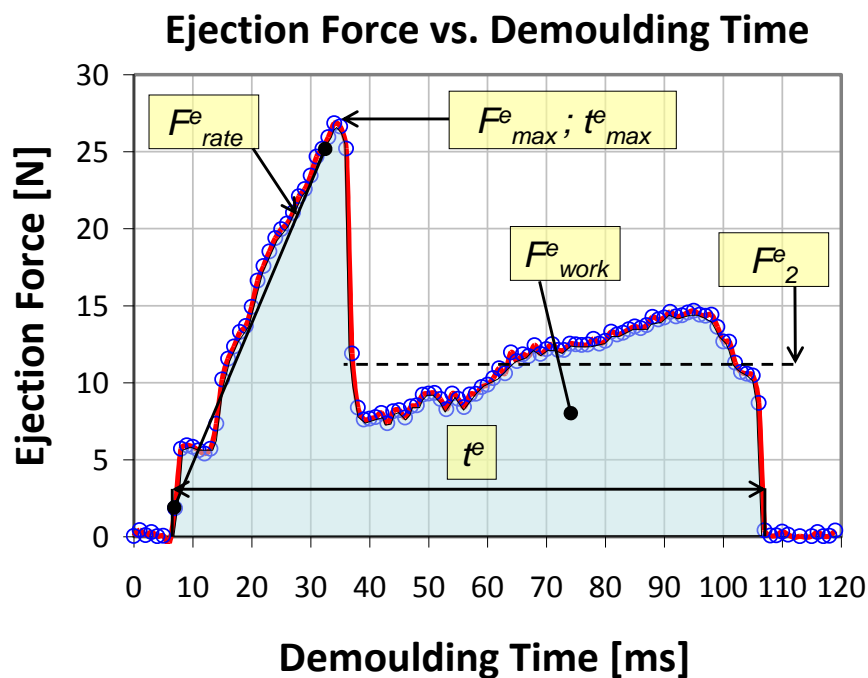

Figure 1. The curve of demoulding force over time

4. Experimental set-up

4.1 Test material

The material used in this research is Topas COC 5013. Topas® is the trade name for Topas Advanced Polymers' cyclic olefin copolymers (COC). COC resins are suitable for the production of transparent mouldings with

applications in optical data storage and optics, e.g. lenses, sensors and other industrial products. The special performance characteristics of this material are: low density, birefringence and water absorption, high transparency, rigidity, strength and hardness. Also, due to its good bio and blood compatibility, COC finds applications in pharmaceutical packaging, medical devices and diagnostic disposable systems. The 5013 grade is characterised by high flowability and excellent optical properties and therefore is recommended for optical and storage media applications where low birefringence and high moulding accuracy are essential.

In µIM the polymer solidification time is much shorter than that in conventional IM due to the high surface-to-volume ratio and therefore the processing requires heated tools. T_m has to be raised to keep the bulk temperature of the polymer sufficiently high to prevent premature solidification of the melt flow in order to ensure complete cavity filling and micro feature replication. On the other hand, T_m should be kept below the specific heat deflection temperature (HDT) of the material in order to preserve dimensional stability and avoid any plastic deformation of the part due to the action of the ejector pin during demoulding. According to the COC material specifications [21], its HDT is 130°C and its mechanical properties decrease with increasing temperature (see e.g. shear modulus in Figure 2) and are maintained until the HDT before dropping sharply after 135°C. The T_m settings used in this research were the minimum and maximum temperature values recommended for COC to allow for good flowability and dimensional stability. The machine used to perform the micro injection moulding of the COC microfluidic systems was a Battenfeld Microsystem 50.
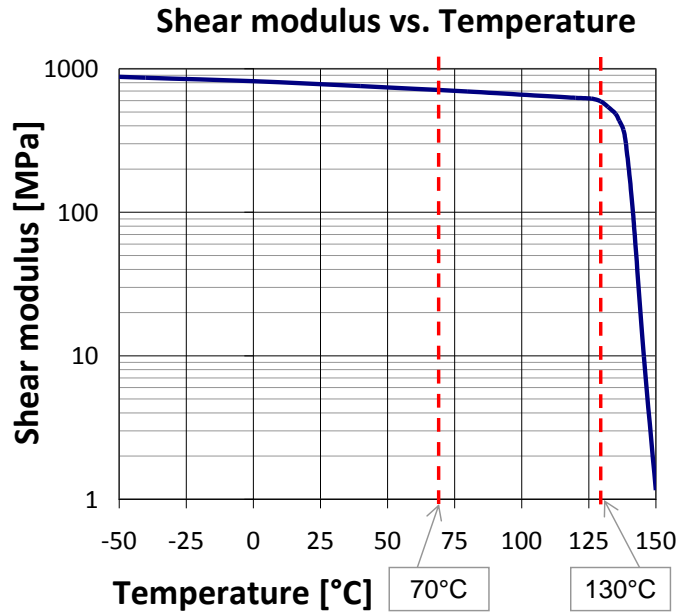
Figure 2. Shear moduls G as function of temperature of the employed COC Topas® 5013 L10: G(70°C) = 700 MPa, G(130°C) = 580 MPa. The low and high mould temperatures adopted in this study are highlighted with red dotted lines [TOPAS2006].

4.2 Part design and tool manufacture

The part design for this study is a micro fluidics platform used in disposable smart diagnostic chips (Figure 3a). The system design comprises a microfluidic channel system with biosensors for the detection of diseases. The overall dimensions of the polymer chip are 10 mm in diameter and thickness of 1 mm. The chip design includes features commonly found in micro fluidics components such as reservoirs and channels. The dimensions of the main channels are width of 50 µm and depth – 80 µm, as shown in Figure 3b. The insert for the µ-IM tool as depicted in Figure 4a was manufactured in steel and produced using conventional turning except for the cavity face micro features that was machined by micro milling. To eject the part a hole is drilled and reamed at the centre of the insert as shown in Figure 4b. The bore accommodates a single 2 mm pin positioned at the centre of the part. A draft angle of 1 degree was applied to each of the features. The tool design incorporates the Battenfeld microsystem 50 machine nozzle into the fixed half

of the mould at the split line and thus to avoid the use of a sprue. The runner has a half round design (2 mm diameter) with a length of 10 mm, an eccentric rectangular gate of 1 x 1 mm and 0.5 mm thickness is used as the part filling entry point. To reduce the influence of the runner surface area on the demoulding force an ejector is positioned in the runner area at the greatest possible distance from the part, so that during the demoulding cycle the gate shears and the part and runner eject separately. The insert was assembled to a primary mould tool and then inspected for parallelism and shut off of the mating faces.
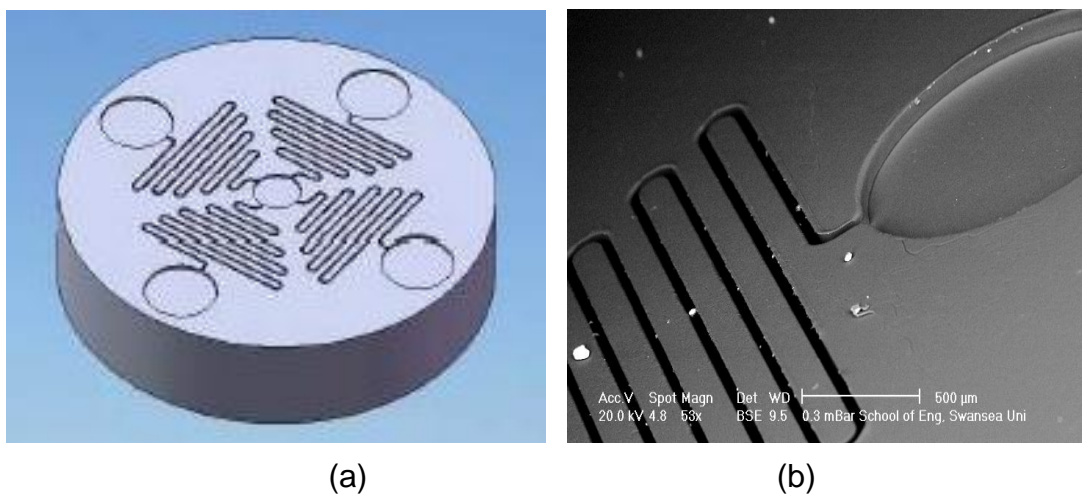

(a)　　　　　　　　　　　　　　　　(b)

Figure 3 (a) Microfluidic part (b) Microfluidic features
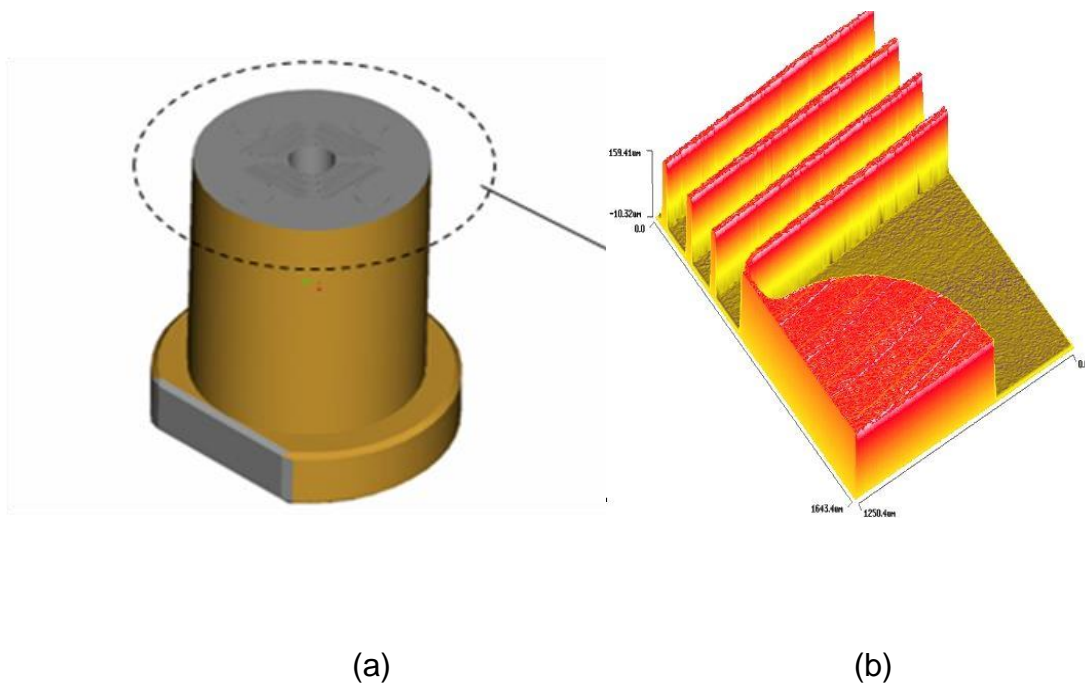

(a)　　　　　　　　　　　　　　　　(b)

Figure 4 (a) mould insert (b) microfluidic features

4.3 Demoulding force measurements

In this study, the variations of F^e during the μ-IM process were analysed. The Kistler 9211B miniature force sensor positioned behind the ejector pin as shown in Figure 5 was used to measure F. To carry out the measurements, the tool was modified to accommodate the ejector pin at the centre of the microfluidic insert. Behind the pin the transducer was positioned on the ejector plate sub assembly. When the ejector assembly moves forward the part is removed from the cavity and the transducer is subjected to a mechanical load that generates an electric potential. The sensors electric charge is then converted using an ICAM Type 5073A Industrial Charge Amplifier. The amplifier is used to set the sensitivity and the range of the sensor, and then converts the piezoelectric charge signal into an output voltage proportional to the mechanical input force. The output signals were monitored with a National Instruments NI 9205 16-bit module. The measurement and output ranges of the charge amplifier were 0 to 10,000 pC and 0 to 10v, respectively. With the ejector pin acting on the transducer, the resulting F^e from the output voltage was calculated. The sensor output signals were then downloaded into a PC using a National Instruments cDAQ-9172 USB data acquisition unit and the measured values, F^e_{Max} F^e_{work} and F^e_{rate}, were accessed through the National Instruments Labview 8 software.

Force sensor behind Ejector Pin

Injection mould (heated, T_m)

Polymer Part

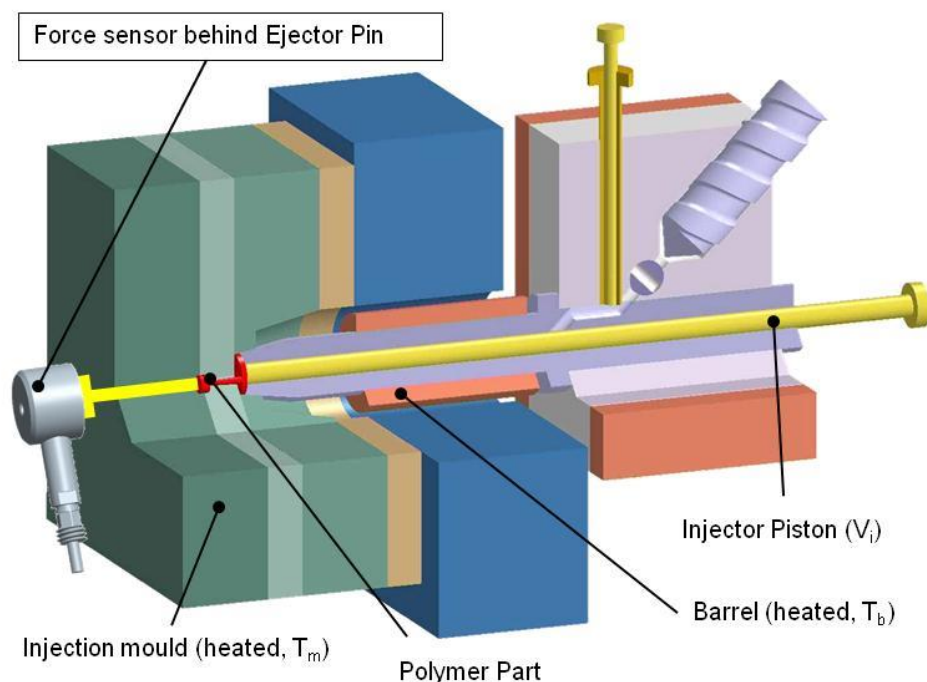Injector Piston (V_i)

Barrel (heated, T_b)

Figure 5. F^e measurement positions

4.5 Design of experiments

The Taguchi design of experiments (DOE) method was used to plan the research with the objectives of: acquiring data in a controlled way, obtaining information about the behaviour of the μ-IM process and also identifying significant factors affecting the process. The sixteen experiments were randomised and by using the DOE signal-to-noise ratio (S/N), which is the ratio between the strength of a signal and the strength of the associated noise, it was possible to identify the process parameters that reduce variability by minimizing the effects of uncontrollable noise factors. In this research the best quality characteristic S/N ratio was considered as a nominal, and it was used to identify those control factors that reduced variability. It was defined as:

$$S/N = 10 \cdot \log_{10}\left(\frac{\bar{y}^2}{s^2}\right) \qquad (5)$$

where Y is the signal and s is the noise.

Further, main effects and interactions effects were calculated for all parameters in relation with the demoulding outputs, and a Pareto analysis was performed. To investigate how process affects the demoulding performance, this experimental research was focused on F^e_{Max}, F^e_{work}, F^e_{rate}, t^e and F^e_2 during the μ-IM process. The pressure and temperature influence during filling stage was controlled by melt temperature (T_b), mould temperature (T_m) holding pressure (P_h) and Injection speed (V_i). Given that four factors at two levels were considered for the selected material, a Taguchi L16 orthogonal array (OA) was selected (Table 1). The melt temperature was controlled through T_b and was within the recommended processing window for COC. In μ-IM the polymer solidification time is much shorter than that in conventional IM and therefore the processing requires heated tools. T_m has to be raised to keep the bulk temperature of the polymer sufficiently high and thus to facilitate the melt flow during the filling stage. The T_m settings used in

this research were the minimum and maximum temperature values recommended for COC.

V_i has two main effects. It can help polymers to fill the cavities before the melt flow solidifies but also it can increase the shear rate of the polymer which results in shear heating, increasing the melt temperature and thus decreasing its viscosity (favourable condition for high surface replication). The low and high levels of V_i selected in this research were chosen by taking into account the replication fidelity of the process and the capability of the Battenfeld Microsystem 50 respectively. In particular, an injection speed of 200 mm/s was selected as the minimum speed providing effective replication at low melt and mould temperatures respectively. The micro injection moulding machine is equipped with an injection piston (with a diameter of 5 mm) for which the maximum injection speed is 946 mm/s over a stroke distance of 84 mm, hence the high level of V_i was selected at 800 mm/s. The two levels of P_h during which P had been maintained were controlled using the Microsystem 50 P_h on and off functions. The holding pressure time (t_h) was set at 10 seconds. Cooling time was set to 5 s in all experiments to ensure that the polymer bulk temperature could reach the mould temperature prior ejection. An ejection speed of 10 mm/s was adopted and set constant during all experiments.

Based on the L16 Orthogonal Array (OA) defined in this way ten trials were performed for each combination of controlled parameters. Thus, 160 experimental trials in total were carried out. The response variables considered were F^e_{Max}, F^e_{work}, F^e_{rate}, t^e and F^e_2.

Table 1. Taguchi L16 Orthogonal Array Design

RUN	Factors			
	COC			
	T_b [ºC]	T_m [ºC]	P^h	V_i [mm/s]
1	240	70	Off	200
2	240	70	Off	800
3	240	70	On	200
4	240	70	On	800

5	240	130	Off	200
6	240	130	Off	800
7	240	130	On	200
8	240	130	On	800
9	300	70	Off	200
10	300	70	Off	800
11	300	70	On	200
12	300	70	On	800
13	300	130	Off	200
14	300	130	Off	800
15	300	130	On	200
16	300	130	On	800

5. Results

5.1 Interval plots for F^e

In this study, a L16 OA was employed, and for each combination of controlled parameters ten runs were carried out and thus ten measurements of F^e_{Max}, F^e_{work}, F^e_{rate}, t^e and F^e_2 were obtained. The mean value plots for each experiment are provided in Figures 6, 7, 8, 9 and 10. The results show that the factors and their respective levels have a varying influence on the process.

F^e_{rate} is defined as the rate from zero F^e to F^e_{max}. The experimental results in Figure 6 clearly show that the control factors affect the mean values. It is shown that experiments 4,8,12 and 16 result in a high F^e_{max} and F^e_{work}. For F^e_{rate}, the same experimental settings lead to a lower F^e_{rate} rate. With F^e_{max} reflecting the maximum force applied and the point at which the part mould seal is broken, the lower F^e_{rate} suggests a more prolonged ejection due to the F^e resistance of the packed part and also a possible part deflection before breaking the seal. This behaviour is also reflected in the ejection time analysis.

The variation of F^e_{max} can be explained with some changes in process conditions due to P_h and V_i, where their high settings result in high F^e_{max} as shown in Figure 7. Additionally, a high V_i with high P^h leads to the four highest F^e_{max} measurements. Similarly, it can be seen in Figure 8 that the experiments 4,8,12 and 16 lead to high F^e_{work} values. These results can be explained with

the high settings for P_h and V_i. It should be noted that for the trials of 3,7,11 and 15, with P_h "on" settings, F^e_{work} is also high.

The interval plot of ejection time (Figure 9) shows the clear effect of melt temperature high settings (experiment from 9 to 16) increasing the ejection time. Additionally, experiments 4, 8, 12, and 16, corresponding to a combination of both applied packing pressure and high injection speed (i.e. high injection pressure) also lead to higher ejection times than when this combination is not present.

Finally, the ejection force of the part after the maximum ejection force is reached shows a slightly lower force when the melt temperature was higher (experiments from 9 to 16) (Figure 10). Particularly high values of F^e_2 are reached when a combination of high mould temperature and applied packing pressure is employed (experiments 7 and 8).
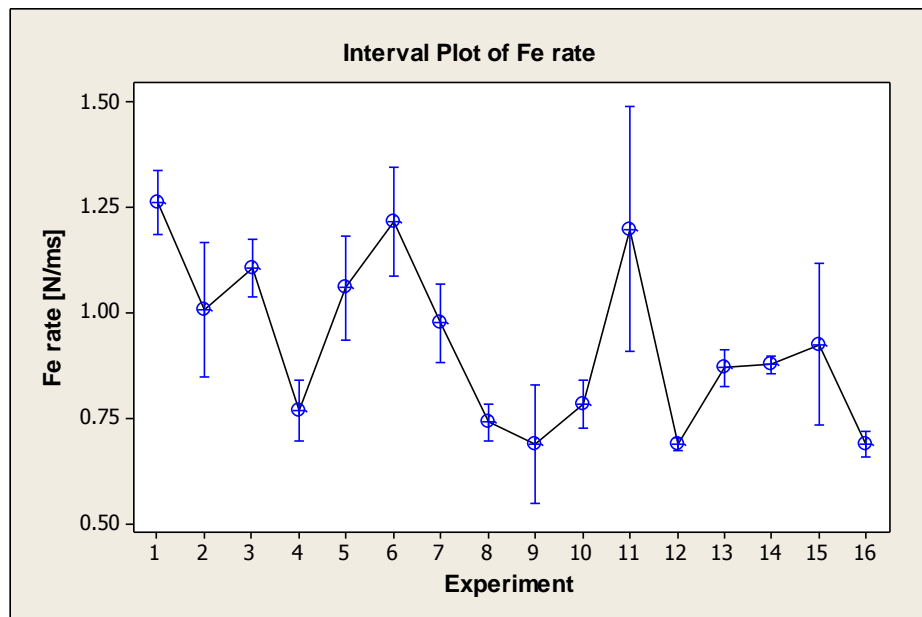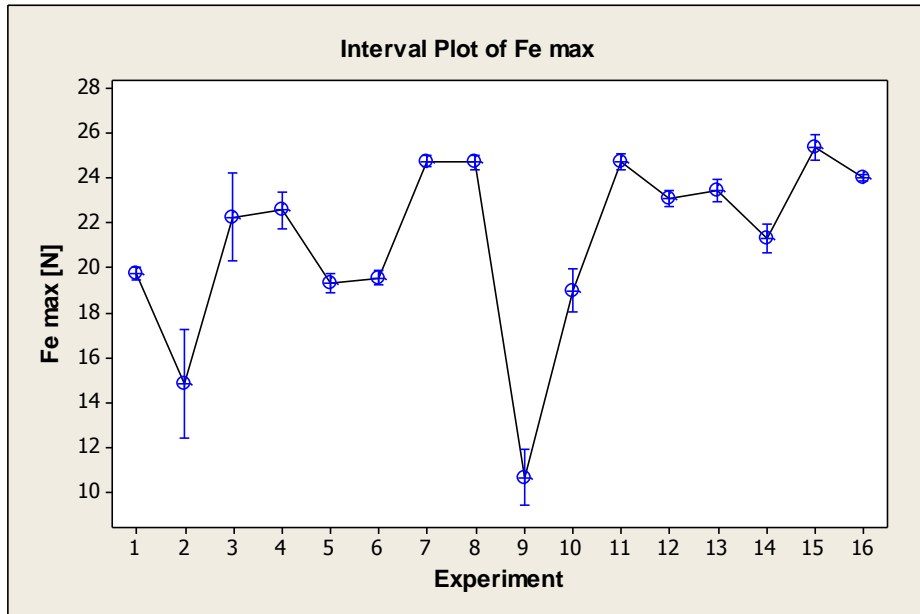

Figure 6. Interval plot of F^e_{rate} results

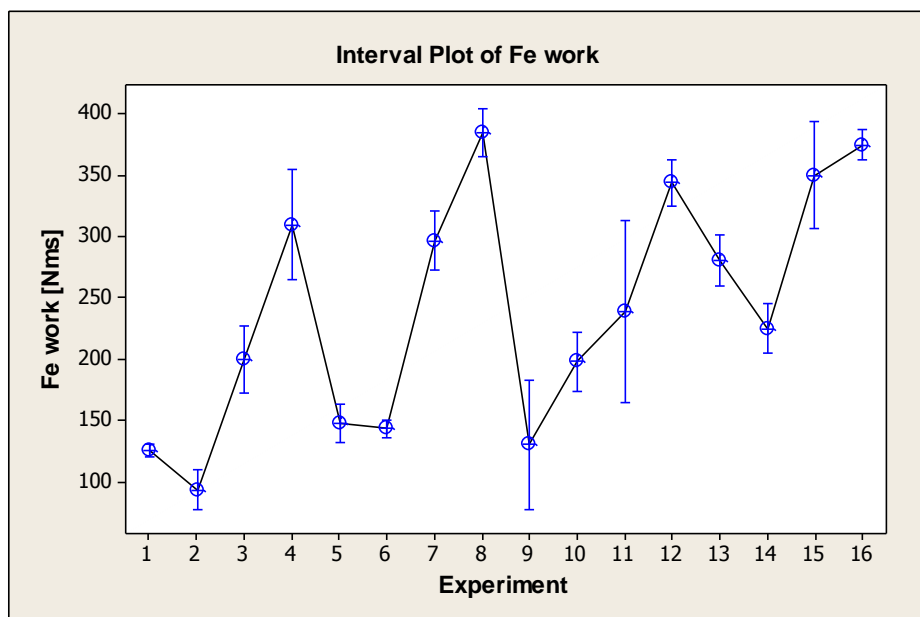Figure 7. Interval plot of F^e_{max} results

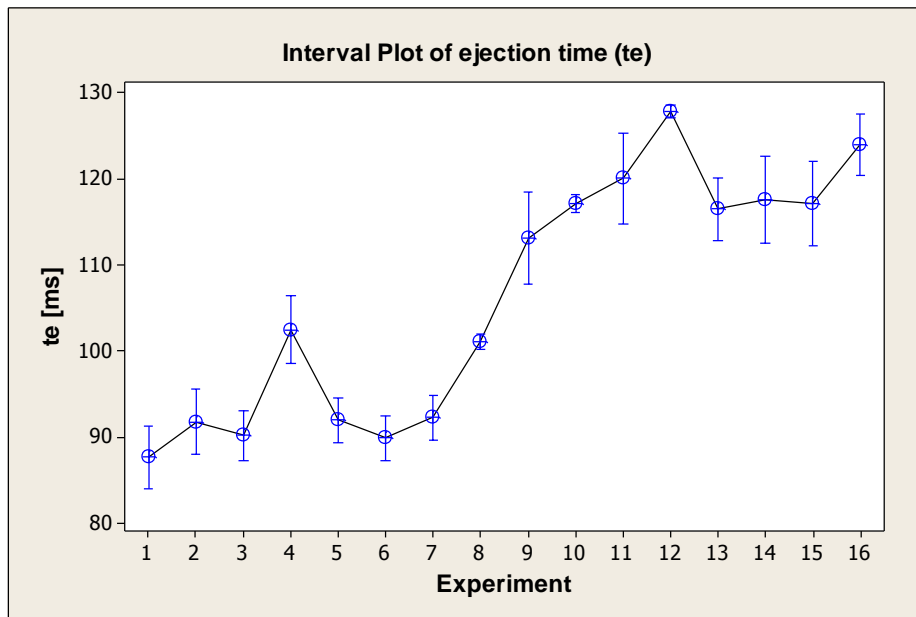Figure 8. Interval plot of F^e_{work}
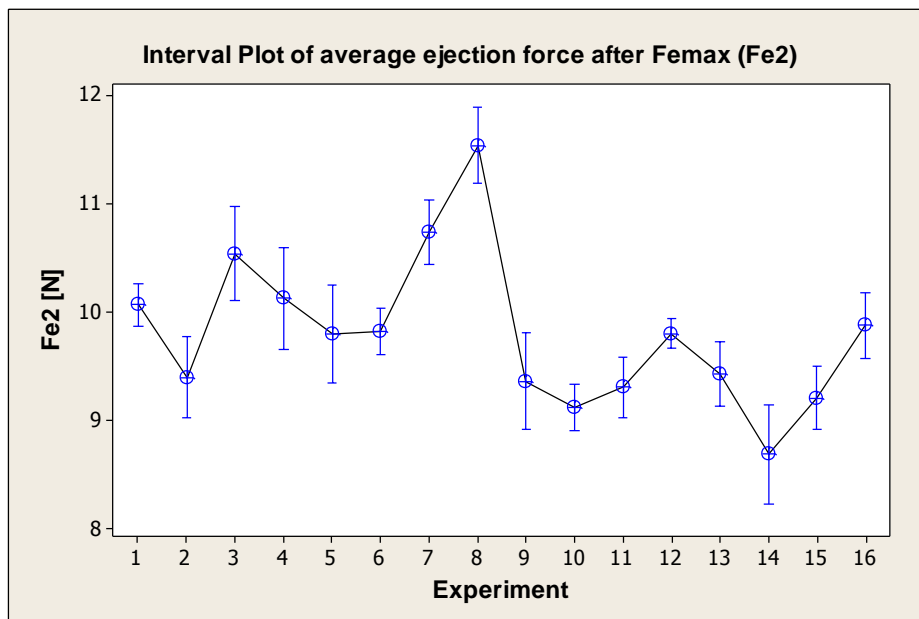
Figure 9. Interval plot of t^e

Figure 10. Interval plot of F^e_2

5.2 Parameters' contribution to F^e.

An analysis of variance (ANOVA) was performed in order to assess the processing parameters' contribution to F^e based on the obtained experimental results. Especially, the parameters' contribution in Table 2 shows their rank importance, percentage contribution, δ statistics, S/N rank importance and S/N δ of each parameter. The S/N values were considered as indicators of

process parameter settings that were resistant to variations due to noise factors.

Table 2. Response table for F^e_{rate} , F^e_{max} and F^e_{work}

Factor	T_b [°C]	T_m [°C]	P^h	V_i [mm/s]
F^e_{rate} response				
Level 1	1.0177	0.9383	0.9712	1.0113
Level 2	0.8407	0.9201	0.8872	0.8471
δ	0.17	0.01	0.08	0.16
Rank importance	1	4	3	2
Level 1	18.14	18.17	18.89	16.34
Level 2	19.94	19.91	19.18	21.74
S/N δ	1.8	1.75	0.29	5.4
S/N Rank importance	2	3	4	1
F^e_{max} response				
Level 1	20.93	19.55	18.47	21.29
Level 2	21.47	22.85	23.93	21.11
δ	0.55	3.3	5.46	0.19
Rank importance	3	2	1	4
Level 1	27.58	24.62	25.80	28.64
Level 2	29.82	32.78	31.60	28.76
S/N δ	2.24	8.16	5.80	0.11
S/N Rank importance	3	1	2	4
F^e_{work} response				
Level 1	212.5	204.9	167.9	220.9
Level 2	267.5	275.2	312.1	259.1
δ	55.1	70.3	144.3	38.1
Rank importance	3	2	1	4
Level 1	18.41	14.44	16.90	15.25
Level 2	16.22	20.19	17.72	19.38
S/N δ	2.2	5.74	0.82	4.13
S/N Rank importance	3	1	4	2

For F^e_{rate}, an increase of all parameter settings results in a F^e_{rate} decrease. This suggests that by increasing the settings of the process factors the part filling and packing improves and thus the resistance to F^e is higher as shown in Figure 11. T_b is the highest rank factor, especially the increase of T_b results in a F^e_{rate} decrease of 16.7 %. With a similar δ value V_i is ranked second in

importance, an increase of V_i results in a F^e_{rate} decrease of 15.8%. In addition, the S/N response of V_i that indicates minimized effects of the noise is ranked first. Thus, for V_i the parameters response high ranking and the high S/N value make it a critical control factor.

The results for F^e_{max} show that P_h has the highest contribution where an increase in the parameter setting results in an increase of 29% (Figure 12). T_m is ranked second with an influence of 17%. Both T_m and P_h have a high S/N δ, thus identifying T_m and P_h as critical control factors that make the process resistant to variation due to noise factors.

For F^e_{work} an increase in the setting results in a F^e_{work} increase (Figure 13), and the responses are ranked with the same importance as F^e_{max}. P_h is dominant as shown by its rank importance and the use of P_h results in a 86% increase in F^e_{work}. Also, like F^e_{max} T_m is ranked second, especially its increase results in an increase of 34% and also T_m has a high S/N δ, which makes it a critical control factor.

The ejection time (t^e) is mainly influenced by T_b. Due to the reduced material rigidity at higher temperature (see Figure 2), the component deforms during ejection while still being engaged in the cavity (Figure 14) and the ejector pin needs a longer time to eject part. Other parameters (such as T_m) also have an influence to this respect, but mainly in the first phase of the demoulding stage, when the ejection of the micro features takes place. This is demonstrated in Figure 15 where the influence of process parameters on the ejection time from start to F^e_{max} is shown. It appears that surface replication is the dominating mechanism from t_{start} until t^e_{max}, whereas a bulk material-related property drives the ejection for the remainder of the ejection time.

Average ejection force in the second phase of the ejection cycle (F^e_2) decreases with increased T_b demonstrating that, once the micro features have been ejected (see Figure 12 for comparison), a less rigid polymer would need a lower force to actually demould the component (see Figure 16).
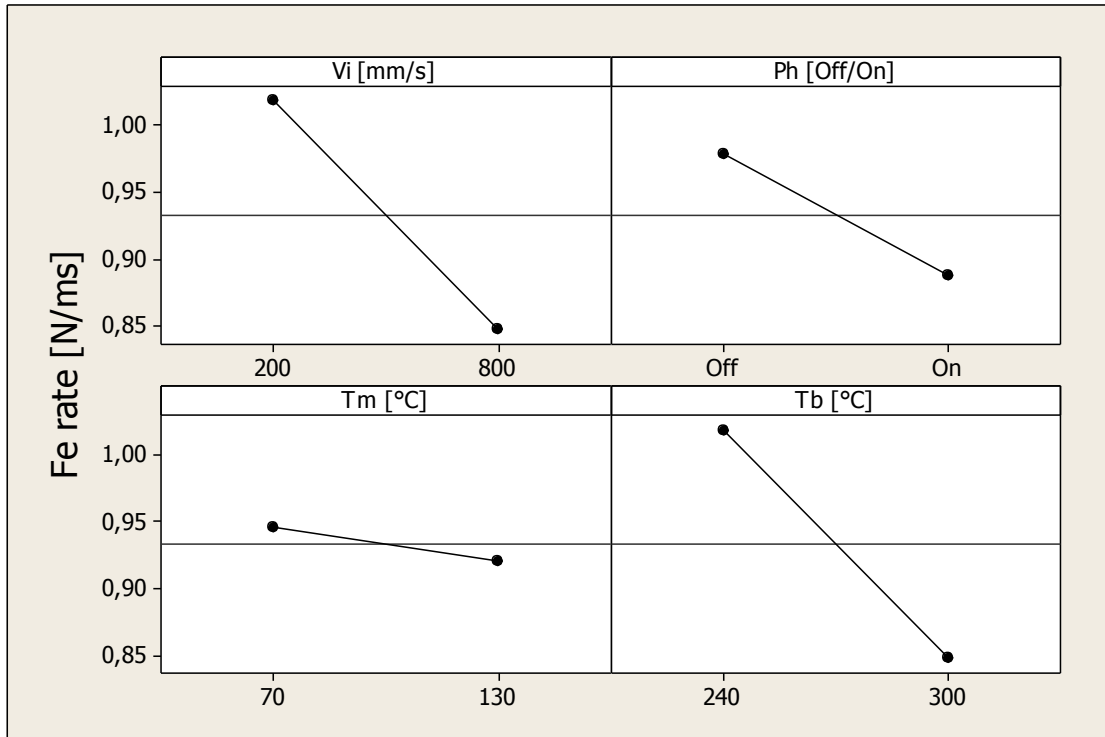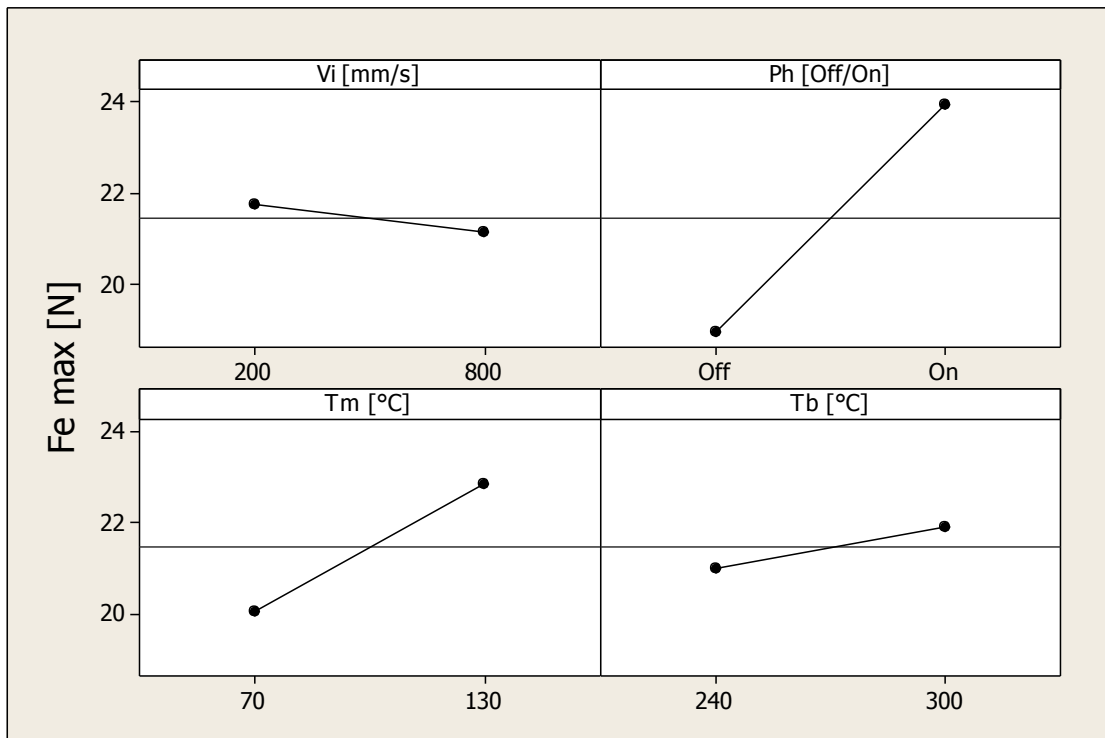
Figure 11. Main effects plot for F^e_{rate}
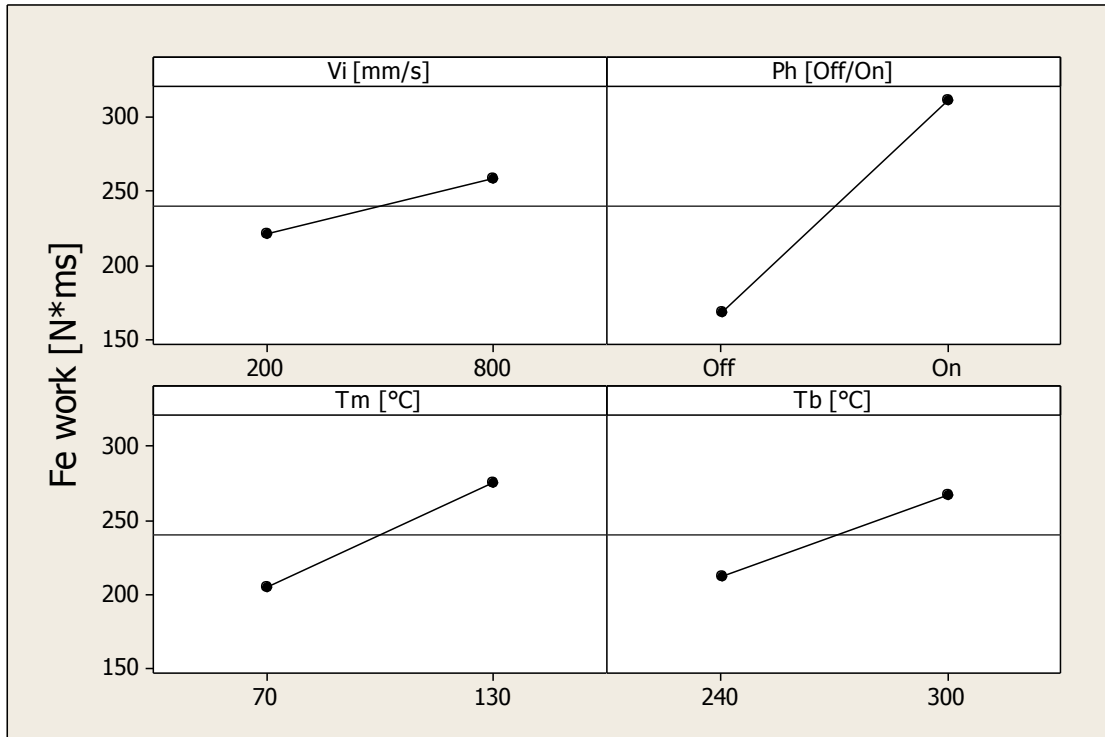

Figure 12. Main effects plot for F^e_{max}

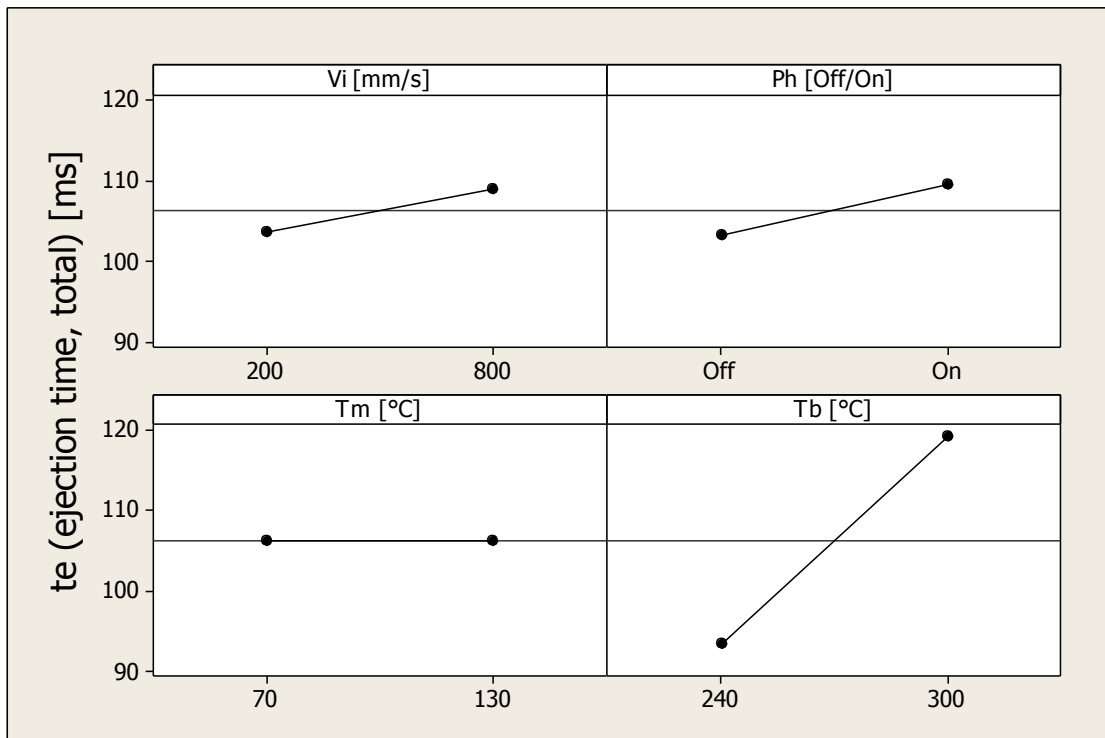Figure 13. Main effects plot for F^e_{work}

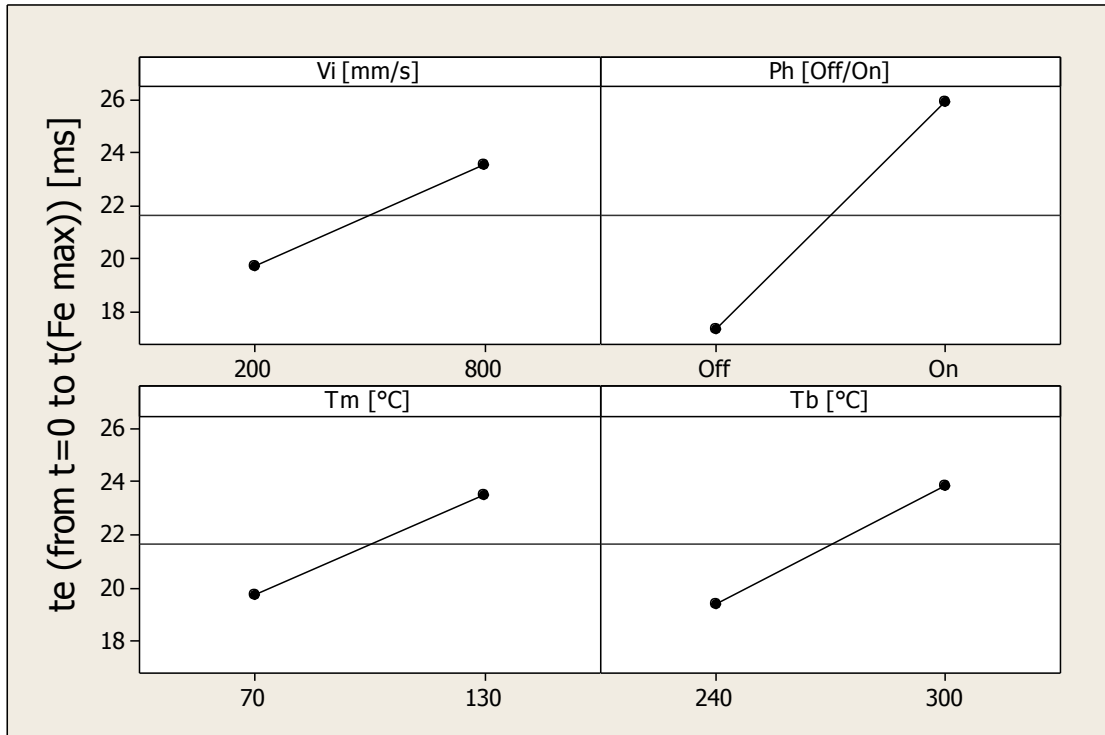Figure 14. Main effects plot for t^e

Figure 15. Main effects plot for t^e from F^e at t=0 to $t(F^e_{max})$.
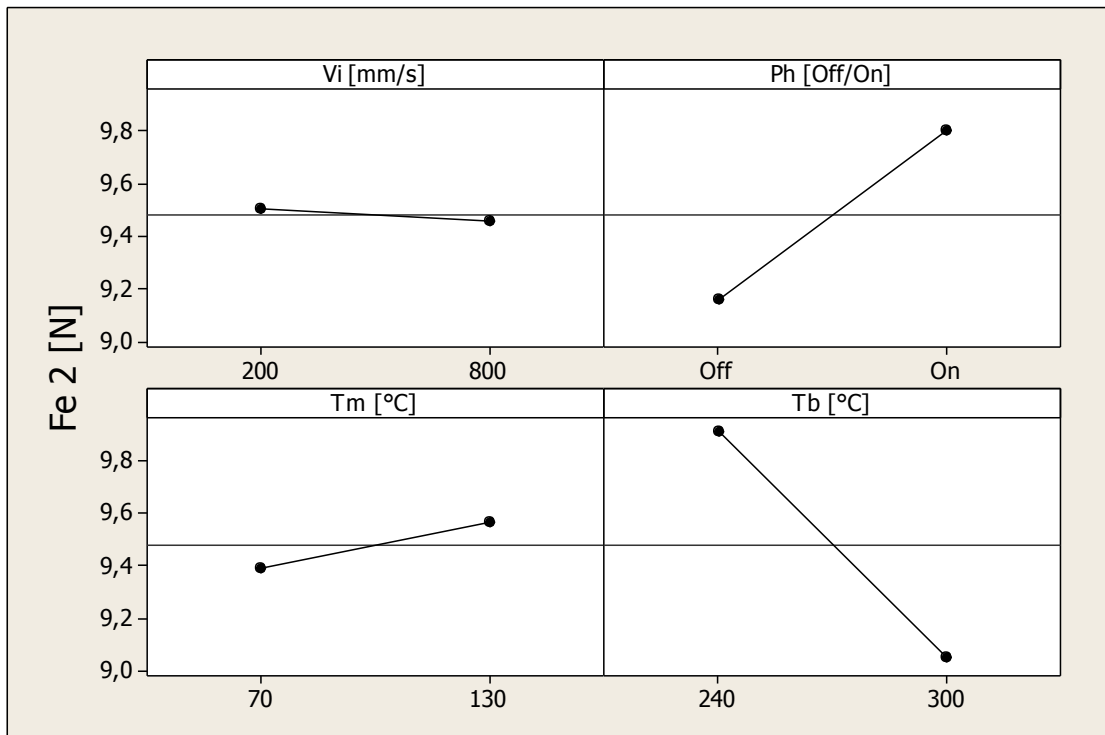

Figure 16. Main effects plot for F^e_2 (average ejection force from $t(F^e_{max})$ until $t(F^e)=0$).

5.3. Factor Interaction analysis

To identify the level of interactions between the variables a Pareto chart of the effects was used to determine the magnitude and the importance of an effect with respect to F^e. The chart x-axis represents the interaction source while y-axis is the magnitude of interaction. It shows the absolute value of the effects and draws a reference line, corresponding to the level of statistical significance (α = 0.05), on the chart. Any effect that extends over this reference line is potentially important and indicates high interactions between the factors. The results are provided in Figures 17, 18 and 19.

By analysing the results, it is immediately apparent that even though there are in some cases significant interactions for F^e_{rate}, F^e_{max} and F^e_{work}, actually no interaction is dominant over all single factors. This is particularly the case for F^e_{max} and F^e_{work}, where the main single factors (presence of holding factor and mould temperature) have a standardized effect at least twice as large as the first significant interaction. However, in Figure 17 it can be seen that for F^e_{rate}, there are two 2-way interactions that have a standardized effect close to that of the main effects of injection speed and melt temperature. In particular, the interaction between injection speed and holding pressure indicates that when both factors are set at high level (i.e. 800 mm/s and 'ON' respectively) the resulting effect is a decrease of the ejection force rate. This can be explained by the joint effect of packing pressure and high injection speed that, by promoting the tool surface replication by the polymer, will cause an increase of the time needed for ejection. A similar effect can be observed for the other interaction between holding pressure and melt temperature. A high mould temperature setting and the presence of holding pressure will promote surface replication, and this in turn will increase ejection time, decreasing the ejection force rate. At the same time the Pareto analysis shows that for F^e_{rate}, injection speed and melt temperature are main factor with the highest effect, as indicated by the main effect plot in Figure 11. Furthermore, for F^e_{max} and F^e_{work} P_h is a significant single factor with the highest effect, as indicated in the main effects plots in Figure 12 and 13.
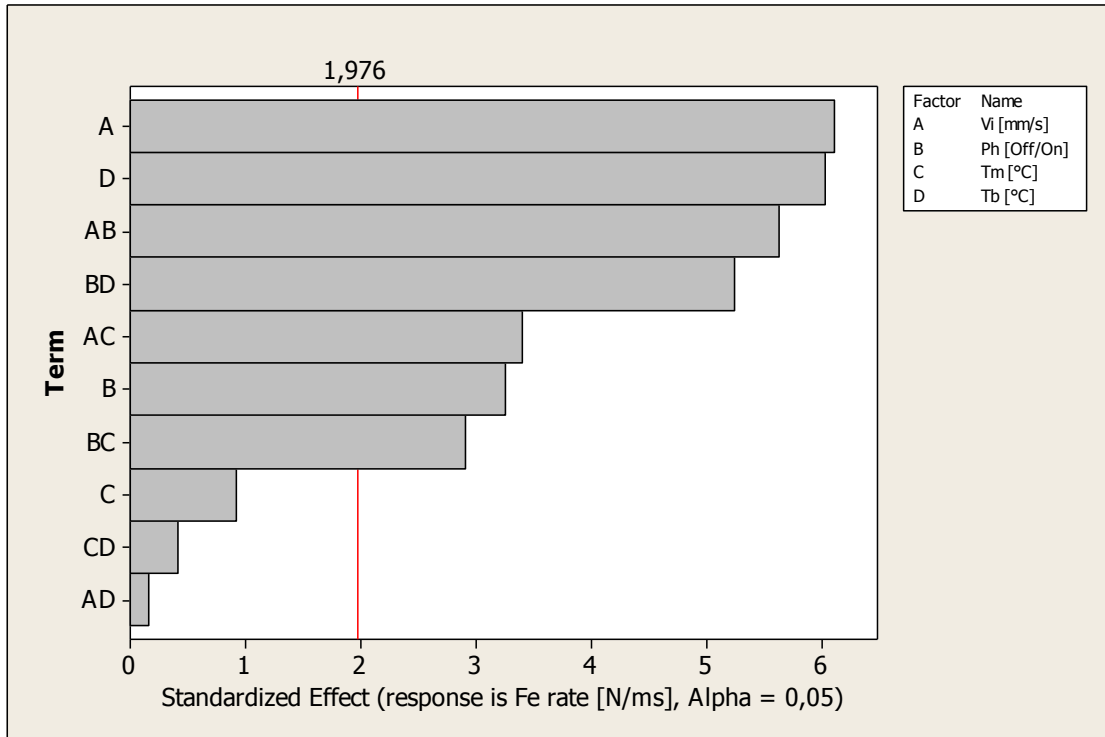
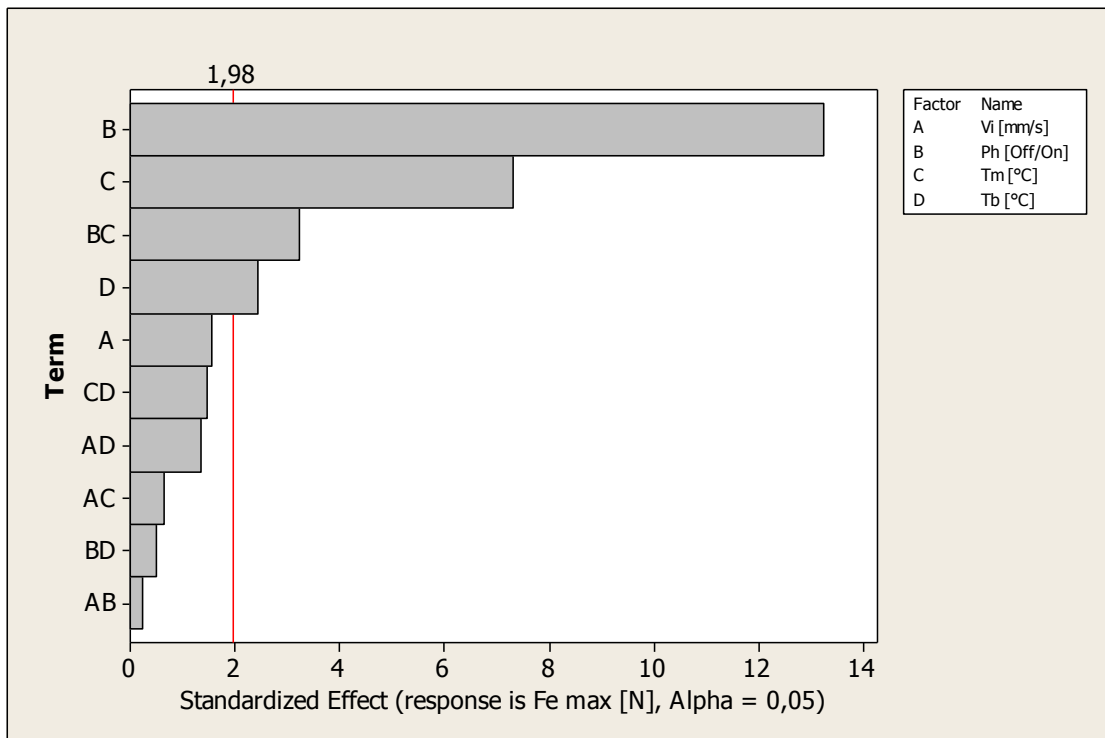Figure 17. Pareto chart of interaction effects for F^e_{rate}

Figure 18. Pareto chart of interaction effects for F^e_{max}
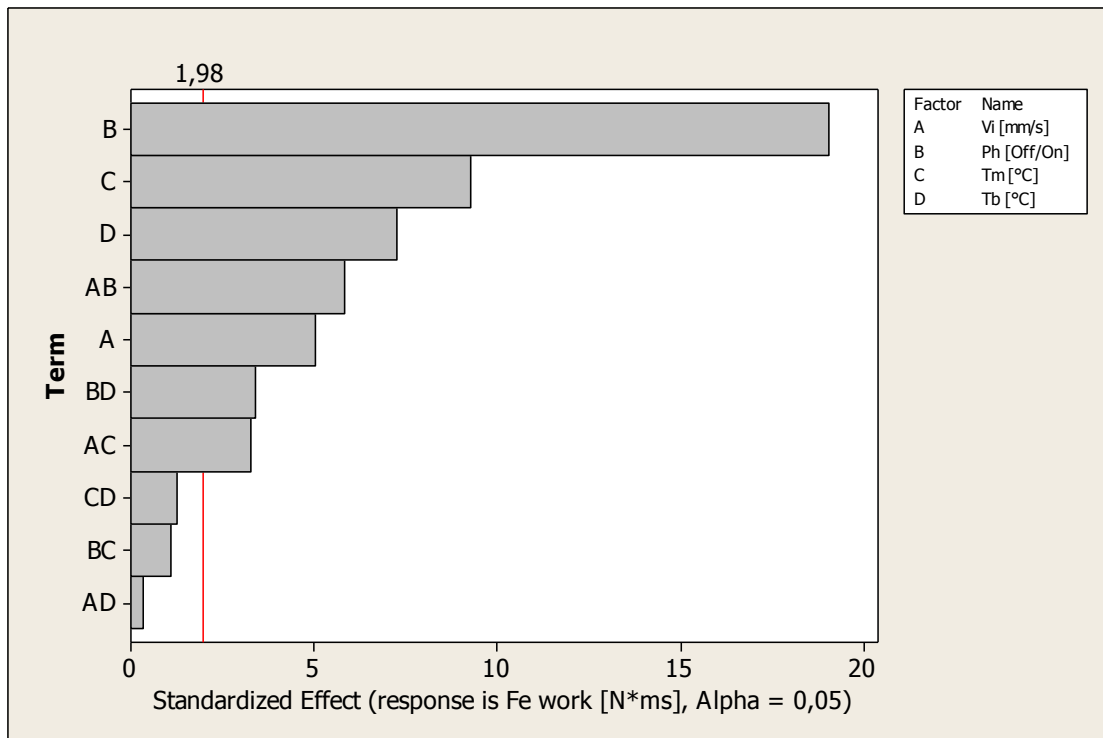
Figure 19. Pareto chart of interaction effects for F^e_{work}

5.4 Optimum parameters levels

The average values of F^e_{rate}, F^e_{max} and F^e_{work} were calculated based on the 10 trials conducted for each combination of control parameters in the OA, and the optimum parameter levels for the investigated polymer, COC, were determined by employing the Taguchi parameter design method [22]. By applying this method it was possible to identify theoretically the best set of µ-IM parameters in respect to F^e within the investigated processing window. For F^e, the value of a given parameter was considered to be the best for the selected two levels, if its corresponding average F^e_{rate} is high while the average values for F^e_{max} and F^e_{work} were the lowest. The theoretical best set of processing parameters is provided in Table 3. From this analysis, it was immediately apparent that in almost every case the low settings of the control parameter levels resulted in process conditions that were optimum for demoulding. The only factor that did not comply with this observation was the V_i setting for F^e_{max} where the high settings led to theoretically lower values. However, for both F^e_{max} and F^e_{work} the respective V_i settings were not unique,

26

as it was shown in Table 2, where V_i had the lowest response of the four factors.

Table 3. The theoretical best set of processing parameters

Resulting	Factor levels for the theoretical high F^e_{rate} and low F^e_{max}, and F^e_{work}				Mean Predicted values
	T_b [ºC]	T_m [ºC]	P_h	V_i [mm/s]	
F^e_{rate}	1	1	1	1	1.16 [N/ms]
F^e_{max}	1	1	1	2	16.2 [N]
F^e_{work}	1	1	1	1	90.53[N·ms]

6. Conclusions

This paper reports an experimental investigation of process parameters' effects on the demoulding conditions in µ-IM. To measure the force required to eject a part a condition monitoring system was designed and implemented. Then, by using the design of experiments approach the demoulding force and its characteristic parameters were studied as a function of four process factors, T_b, T_m, P_h and V_i. The main conclusions made based on the obtained results are:

- It was shown that F^e_{rate}, F^e_{max}, F^e_{work} , t^e and F^e_2 were dependent on the processing conditions. Hence, by monitoring F^e , the force exerted on the part can be adjusted by acting on the µ-IM process settings.

- Significant variations between the trials in different processing conditions were observed and there was a direct correlation between the applied pressure during the part filling and holding phases of the µ-IM cycle and the demoulding force. The mean value plots for each experiment show that the control factors had a varying influence on the process. The maximum force, F^e_{max}, the point at which the part mould seal is broken, is clearly influenced by P_h and T_b. The same two process parameters influence F^e_{work}, which represents better the overall force acting on the part over the demoulding phase. For F^e_{rate}, the effects of T_b and V_i

influence the rate of part removal. Especially, a more prolonged ejection can be explained with the effects of better filled and packed mould cavities that resist F^e and possibly causing a part deflection before breaking the part mould seal. This was demonstrated through the ejection time analysis. Further, the ejection force after its maximum has been reached was influenced by the melt temperature, confirming that the dependence of the polymer mechanical property with the temperature is of primary importance when dealing with demoulding as well as µ-IM settings.

- The Pareto analysis of control parameters' interactions showed the main effects of the investigated process factors had the highest standardized effect and confirmed the DOE main effect analysis. Few 2-ways interaction had significance however there was no interaction more dominant than the single factors. In particular, for F^e_{rate} there were two interactions with particularly high standardized effects closer to those of single factors: the interaction effects between P_h and V_i, and between T_b and V_i.

- Ejection force work (F^e_{work}), is mainly determined by Ph and Tb, showing that higher settings of these two parameters can lead to a situation where an overall higher ejection force needs to be applied for a longer time, potentially increasing the risk of deformation.

- As it can be expected F^e is high when the polymer temperature is raised high enough for the full part filling and when a holding pressure is applied to the part. The maximum ejection force (F^e_{max}) is strongly dependent on moulding factors that typically enhance surface replication (Tm, Tb), i.e. that increase friction due to polymer interlocking at the surface of the micro tool. Higher stresses are induced by Ph, which also contribute to higher ejection forces.

In summary, as far as the polymer replication fidelity and dimensional stability is concerned, there is no doubt that high settings of process parameters (i.e. Tm, Tb, Vi, Ph) are advantageous, but there is a point when they start affecting the

ejection phase by increasing F^e significantly, determining a conflict of interest to obtain high performance processing and high quality products in microinjection moulding. Together with well designed ejection systems and optimum tool surfaces a theoretical best set of processing parameters based on condition monitoring can be identified to avoid an excessive F^e and thus prevent quality issues during the μ-IM process.

ACKNOWLEDGMENTS

REFERENCES

[1] Chen, S.C., Chang, Y., Chang, Y.P., Chen, Y.C., and Tseng, C.Y., 2009, Effect of cavity surface coating on mold temperature variation and the quality of injection molded parts International Communications in Heat and Mass Transfer, 36(10), pp.1030–1035.

[2] Lucchetta, G., and Bariani, P.F., 2010, Sustainable design of injection moulded parts by material intensity reduction, CIRP Annals - Manufacturing Technology, **59**(1) pp.33–36.

[3] Shen, C., Wang, L., and Li, Q., 2007, Optimization of injection molding process parameters using combination of artificial neural network and genetic

algorithm method, Journal of Materials Processing Technology, **183**(2-3), pp.412–418.

[4] Ogilvie, R.G., Sieben, V.J., Floquet, C.F.A., Zmijan, R., Mowlem, M.C., and Morgan, H., 2010, Reduction of surface roughness for optical quality microfluidic devices in PMMA and COC, J. Micromech. Microeng, **20**(6) pp.065016-065024.

[5] Dhouib, K., Malek, C.K.,,Pfleging, W., Gauthier-Manuel, B., Duffait, R., Thuillier, G., Ferrigno, R., Jacquamet, L., Ohana, J., Ferrer J.L., Theobald-Dietrich, A., Giege, R., Lorbera, B., and Sauter, C., 2009, Microfluidic chips for the crystallization of biomacromolecules by counter-diffusion and on-chip crystal X-ray analysis, Lab Chip, **9**(10), pp.1412–1421.

[6] Schütte, J., Freudigmann, C., Benz, K., Jan Bottger Gebhardt R., and Stelzle M., 2010, A method for patterned in situ biofunctionalization in injection-molded microfluidic devicesJulia Lab Chip,**10**, pp.2551–2558.

[7] Chen, C.S., Chen, S.C., Liao, W.H., Chien, R.D., and Lin, S.H., 2010, Micro injection molding of a micro-fluidic platform, International Communications in Heat and Mass Transfer, **37**(9), pp.1290–1294.

[8] Chen, S.C., Wang, Y.C., Liu, S.C., and Cin J.C., 2009,Mold temperature variation for assisting micro-molding of DVD micro-featured substrate and dummy using pulsed cooling, Sensors and Actuators. A Physical, **151**(1) pp.87-93.

[9] Chen, S.C., Chang, Y., Chang, T.H., and Chien, R.D., 2008, Influence of using pulsed cooling for mold temperature control on microgroove duplication accuracy and warpage of the Blu-ray Disc, International Communications in Heat and Mass Transfer, **35**(2), pp.130–138.

[10] Lin, H.Y., Chang, C.H., and Young., W.B., 2010, Experimental and analytical study on filling of nano structures in micro injection molding,

International Communications in Heat and Mass Transfer, **37**(10), pp.1477–1486.

[11] H.N. Hansen, R. Hocken, G. Tosello, Replication of micro/nano geometries, 2011, Annals of CIRP (International Academy for Production Engineering), Vol. 60(2), pp. 695-714.

[12] Panchal, R.R., and Kazmer, D.O., 2010, In-Situ Shrinkage Sensor for Injection Molding, Journal of Manufacturing Science and Engineering, **132**(6), pp.064503-064509.

[13] Delaunay, D., Le Bot, P., Fulchiron, R., Luye, J.F., And Regnier, G., 2000, Nature of Contact Between Polymer and Mold in Injection Molding. Part II: Influence of Mold Deflection on Pressure History and Shrinkage, Polymer Engineering and Science, **40**(7), pp.1692-1700.

[14] V. Leo and Ch. Cuvelliez, 1996, The Effect of the Packing Parameters, Gate Geometry, and Mold Elasticity on the Final Dimensions of a Molded Part, Polymer Engineering and Science, Vol. 36(15), pp.1961-1971.

[15] Griffiths, C. A., Dimov, S.S., Scholz, S, Tosello, G. 2011, Process factors influence on cavity pressure behaviour in micro-injection moulding. *ASME Transactions, Journal of Manufacturing Science and Engineering,* **133**(3), pp. 031007,1-10.

[16] Chen, S.C., Chang, J.A., Hsu, W.Y., Sung, W., and Huang, S,W., 2011, Improvement of replication accuracy of micro-featured molding using gas-assisted heating for mold surface, Microelectronic Engineering, **88**(7), pp. 1594-1600.

[17] Griffiths, C.A., Dimov, S.S., Brousseau, E.B., Chouquet, C., Gavillet, J., and Bigot, S.,2009, Investigation of surface treatment effects in micro-injection-moulding**,** The International Journal of Advanced Manufacturing Technology, **47**(1-4), pp.99-110.

[18] Ong, N.S., Koh, Y.H., and Fu, Y.Q., 2002, Micro lens array produced using hot embossing process, Microelectronic Engineering, **60**(3-4). pp. 365–379.

[19] Kim, S.K., Choi, S.J., Lee, K.H., Kim, D.J., and Yoo, Y.E., 2010,Observation of Instabilities in Flow Front During Micro Injection Molding Process, Polymer Engineering & Science Volume, **50**(7), pp.1377–1381.

[20] Zhang, H.L., Ong, N.S., and Lam Y.C., 2008, Experimental Investigation of Key Parameters on the Effects of Cavity Surface Roughness in Microinjection Molding, Polymer Engineering and Science, **48**(3),pp.490-495.

[21] Topas Advanced Polymers GmbH (Frankfurt am Main, Germany), 2006, TOPAS Cyclic Olefin Copolymers (COC) – Product brochure, 20 pp., http://www.topas.com/ (accessed on December 2013).

[22] D. Montgomery, Design and Analysis of Experiments, 6th edition, Wiley (2004), ISBN: 047148735X, pp.1-450.